

The influence of short time heat treatment on the magnetic behaviour of $\text{SmCo}_5/\alpha\text{-Fe}$ nanocomposite obtained by mechanical milling

R. HIRIAN^{1,2,*}, S. MICAN¹, O. ISNARD^{3,4}, V. POP¹

¹Faculty of Physics, Babeş-Bolyai University, Cluj-Napoca, RO-400084, Romania

²MedFuture Research Center for Advance Medicine, "Iuliu Hațieganu" University of Medicine and Pharmacy, L. Pasteur 4-6, 400349 Cluj-Napoca, Romania

³University Grenoble Alpes, Institut NÉEL, 25 rue des martyrs, F-38042 Grenoble, France

⁴CNRS, Institut NÉEL, 25 rue des martyrs, F-38042 Grenoble, France

Exchange coupled nanocomposite hold great promise for the future of permanent magnets, with a predicted energy density of 1 MJ/m^3 . However, due to the precise nanostructure control required, compaction at high temperature can pose difficulties. In this work we explore the effects of high temperature annealing, up to $820 \text{ }^\circ\text{C}$ (for a short duration), on the magnetic properties of exchange coupled $\text{SmCo}_5+20\%\text{Fe}$ nanocomposite powders produced through mechanical milling. These results were compared to those obtained for samples annealed at lower temperature for a longer duration (up to 1.5 h). In both cases promising energy products (estimated for the 100% dense samples) of approximately 100 kJ/m^3 have been obtained, for certain annealing regimes in isotropic samples.

(Received December 6, 2021; accepted December 6, 2022)

Keywords: magnetic nanocomposites, spring magnet, short time annealing, mechanical milling

1. Introduction

Permanent magnets are crucial components in many modern day applications. However the highest performing materials are based on rare earth elements such as Dy, Sm and Nd. These lanthanides elements are mined and processed only in specific regions on the globe; therefore the supply of rare-earths is tenuous and can lead to market crashes, as has happened in recent memory [1, 2]. There is a concerted effort to alleviate our dependence on these types of materials, with efforts like recycling [3], searching for new highly anisotropic materials which do not contain rare earths [4] and exchange coupled nanocomposites [5].

In exchange coupled nanocomposites the high magnetic moment of a soft magnetic material is stiffened by the high anisotropy of a hard magnetic material through the exchange interaction. In order to obtain a good degree of interphase exchange coupling, the sizes of the soft magnetic inclusions must be kept below twice the domain wall length of the hard magnetic phase [5, 6]. Thanks to the presence of soft magnetic phases with high magnetization, exchange coupled nanocomposites have been predicted to be able to store twice the energy of the current generation of high performance permanent magnets [7]. Moreover, the addition of a soft magnetic phase, like Fe or Co increases the corrosion resistance of the final material (as compared to the hard magnetic phase alone) [8]. These types of materials have been successfully created or consolidated so far by using a variety of synthesis methods: melt-spinning [9], mechanical milling

(MM) [10, 11], sono-chemical synthesis [12], bulk injection casting [13], suction casting [14], spark plasma sintering [15-17], hot deformation [18], thin films [19]. the latter being the most successful attempt, with obtained energy products of over 400 kJ/m^3 .

In the case of SmCo_5+Fe spark plasma sintered (SPS) compacts, obtaining dense compacts requires both high pressure and high temperature. However high temperatures treatments of SmCo_5+Fe composites lead to the growth and germination of $\text{Sm}_2\text{Co}_{17}$ impurity phase (some quantity of which is formed as early as the milling stage) [16, 20, 21, 22, 23] which is generally believed to lower the magnetic performance. Therefore in this work we studied the effect of high temperature annealing, up to $820 \text{ }^\circ\text{C}$, for short durations on $\text{SmCo}_5+20\%\text{Fe}$ nanocomposite powders, in order to investigate the feasibility of sintering exchange coupled nanocomposites at such high temperature while preserving the microstructure required for effective interphase exchange coupling.

2. Experimental details

The SmCo_5 ingot was produced by induction melting and subsequent annealing at $950 \text{ }^\circ\text{C}$ for 72 h under purified Ar atmosphere. The starting powder was made by mixing the crushed and sieved SmCo_5 alloy (particle size $< 500 \text{ }\mu\text{m}$) with 20 wt% commercial NC 100.24 Fe powder (particles size $< 100 \text{ }\mu\text{m}$). The mixture was dry milled in a Fritsch Pulverisette 4 planetary ball mill, under Ar gas, for

6 hours using $\varnothing = 10$ mm diameter steel balls. The milling vials and balls are made of 440C hardened steel. The ratio between the rotation speed of the disk and the absolute rotation of the vials was $\Omega/\omega = 333$ rpm/- 566 rpm with a ball to powder weight ratio of 10:1. The milled powder was then wrapped in tantalum foil, sealed in a quartz tube under Ar atmosphere and annealed. Annealing was done at different times and temperatures: relatively long duration annealing was performed for 1.5 h at 500 °C, 550 °C and 0.5 h at 600 °C, while short time annealing was performed for 1.5 min at temperatures between 700 °C and 820 °C. The structure and microstructure of the annealed samples was investigated by X-ray diffraction (XRD) using a Bruker D8 Advance diffractometer equipped with a Cu $\lambda=1.5418\text{\AA}$ source and Bragg – Brentano focusing geometry. The mean crystallite sizes were evaluated through the Scherrer [24] method from XRD patterns. To this end higher resolution patterns were recorded around the investigated peak positions (not shown). The full width at half maximum (FWHM) of the α -Fe ($2\theta = 82.3^\circ$) and SmCo₅ ($2\theta = 30.5^\circ$) peaks was determined by fitting the peaks with the sum of two Pseudo-Voigt functions of the same shape and an intensity ratio of 0.5, corresponding to

the Cu-K α_1 and Cu-K α_2 components of the X-ray radiation. The crystallite sizes and volume fraction for the soft magnetic phase were also checked by Rietveld refinement on the full patterns. Because the evaluations were made on annealed samples, the influence of internal stress on the FWHM was neglected. For magnetic measurements, the powder samples were immobilized in epoxy resin. The demagnetization curves were recorded at room temperature using the extraction method in applied fields up to 10 T. The calculations for the internal field H_{int} were done in the approximation of isolated spherical particles taking into account a mean demagnetization factor of 1/3. The reported values are normalized to the mass of the magnetic powder, and $(BH)_{max}$ is extrapolated for fully dense samples.

3. Results and discussion

We would like to point out the fact that the results, discussed in this section are also partially discussed in the PhD. Thesis of R. Hirian [25].

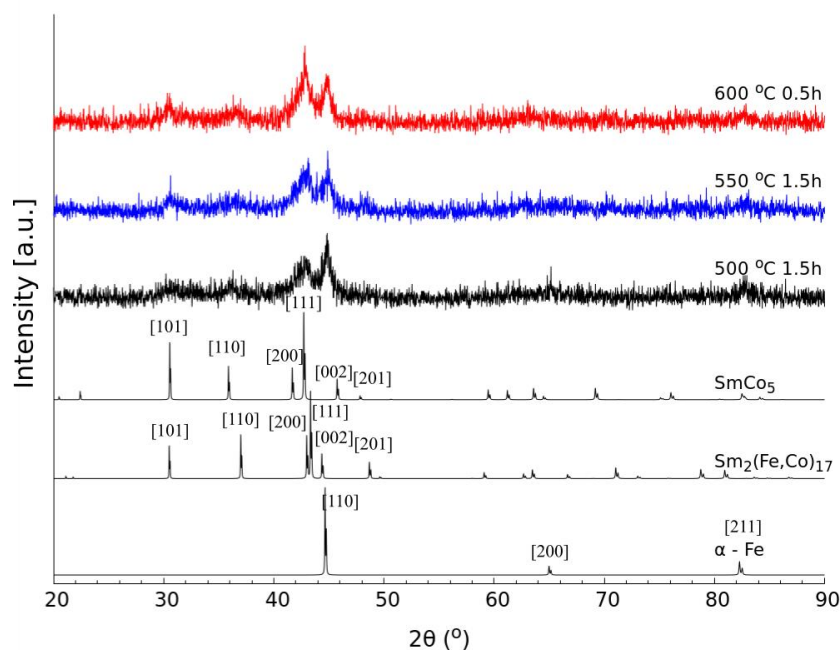


Fig. 1. Normalized XRD patterns for the SmCo₅+20 wt% α -Fe nanocomposite milled for 6 h and annealed at 500, 550 and 600 °C for 1.5 h and 0.5 h respectively. Calculated XRD patterns for SmCo₅, 2:17 and Fe phase are also given. Diffraction patterns are also presented in previous work [11] (color online)

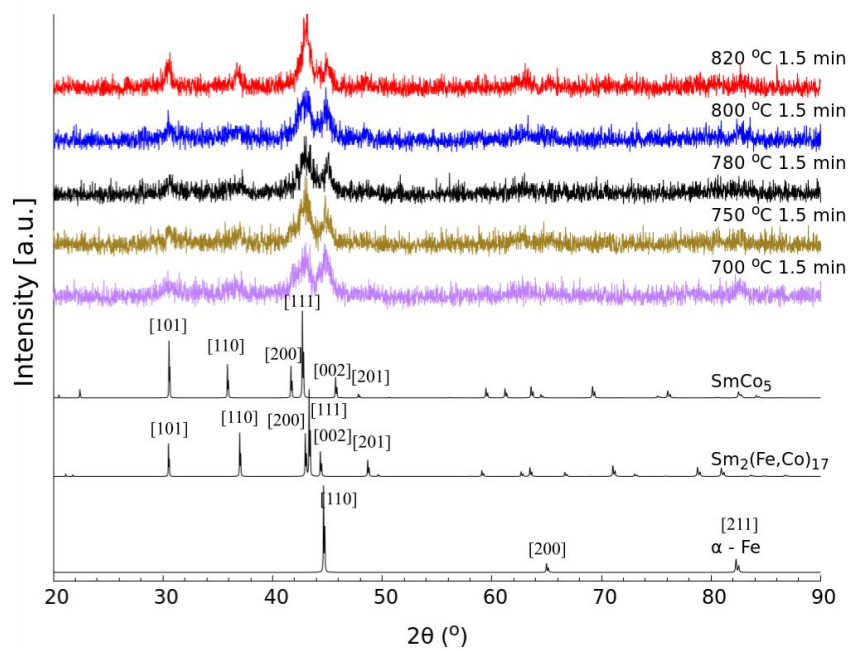


Fig. 2. Normalized XRD patterns for $\text{SmCo}_5+20 \text{ wt}\% \alpha\text{-Fe}$ nanocomposites milled for 6 h and short time (1.5 min) annealed at temperature between 700 and 820 °C. Calculated XRD patterns for SmCo_5 , 2:17 and Fe phase are also given (color online)

XRD patterns were recorded for both classically annealed and short time annealed samples, Fig. 1 and Fig. 2, respectively. Both annealing regimes have proven effective in the recovery of the hard magnetic phase with the peaks attributed to the SmCo_5 and $\alpha\text{-Fe}$ phases being clearly visible, Figs. 1 and 2.

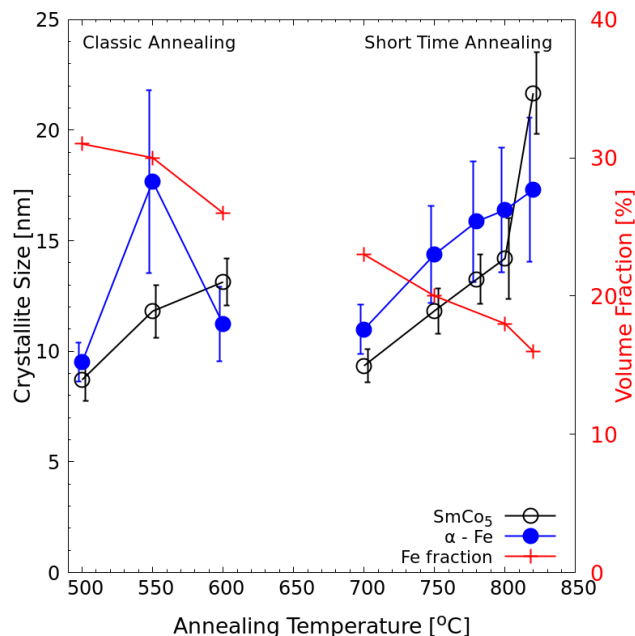


Fig. 3. Average crystallite sizes vs. annealing temperature for the 6 h MM $\text{SmCo}_5 + 20 \text{ wt}\% \alpha\text{-Fe}$ nanocomposite samples. Samples were annealed for 1.5 h at 500 and 550 °C, 0.5 h at 600 °C and 1.5 min at 700 - 820 °C. The estimated volume fraction of Fe as a function of temperature is also plotted (right axis) (color online)

Moreover the peaks attributed to the hard magnetic phase become better defined with increasing temperature for both types of heat treatment. However, we must note that in the case of the sample annealed at 820 °C we can also make out peaks belonging to the $\text{Sm}_2\text{Co}_{17}$ structure.

The crystallite sizes for the annealed nanocomposite samples, estimated from XRD, are shown in Fig. 3. We can see that for the long time annealing, raising the temperature from 500 to 550 °C produces a large increase in the average crystallite sizes for $\alpha\text{-Fe}$, but only a small increase in the case of the SmCo_5 phase. However further increasing the annealing temperature while lowering the duration, from 1.5 h at 550 °C to 0.5 h at 600 °C, the crystallite sizes can be kept in check (Fig. 3). For short time annealing, crystallite sizes vary linearly with annealing temperature, with the exception of the point measured at 820 °C when the measured average size for the hard magnetic phase suddenly jumps to a much higher value. This sharp increase could be due, at least in part, to the convolution with the $\text{Sm}_2\text{Co}_{17}$ phase. Due to the large FWHM values in the recorded XRD patterns, the peaks for the two hard magnetic phases are highly overlapping and therefore hard to quantitatively evaluate. All in all, all samples present a microstructure favourable for the achievement of a good degree of magnetic interphase exchange coupling i.e. Fe crystallite sizes are kept in the 5 - 20 nm range. The evolution of the 2:17 phase was indirectly investigated, using the volume fraction of Fe. From Fig. 3, we can see that the volume fraction of Fe, estimated by full pattern refinement, goes down with increasing temperature. This behaviour is attributed to the growth and formation of the 2:17 phase, i.e. $\text{SmCo}_5+\text{Fe} \rightarrow \text{Sm}_2(\text{Co,Fe})_{17}$. For the short time annealed samples, we see a linear decrease in the quantity of Fe phase, up to 800 °C, after which the slope changes abruptly. The sudden

decrease in the quantity of Fe correlates well with the explanation that the sudden jump in the crystallite sizes of the soft magnetic phase is actually due to the convolution between Fe and 2:17 patterns.

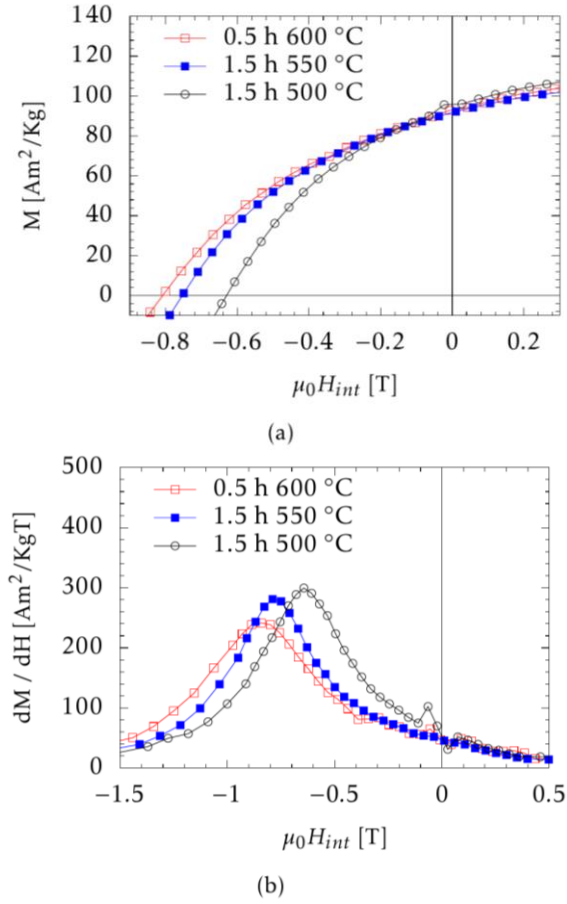


Fig. 4. Demagnetization curves (a) and dM/dH vs H plots (b) for SmCo₅ + 20 wt% α-Fe nanocomposites 6 h MM and annealed at 500 - 600 °C for 0.5 or 1.5 hours (color online)

The magnetic properties for both data sets, long and short time annealing respectively, were investigated through demagnetization curves and dM/dH vs H plots. From the demagnetization curves (Fig. 4a) we can see that for the long time annealed samples, remanence varies little for all samples, while coercive field H_c increases with annealing temperature. A similar trend is observed for the rapidly annealed samples (Fig. 5a), however in this case we also notice an improvement in the rectangularity of the curves with increasing annealing temperature. This behaviour could be explained by the better crystallinity of the hard magnetic phase by increasing the heat treatment temperature. Moreover this behaviour is confirmed by the derivative of the magnetization vs. field (Figs. 4b and 5b) where in the case of the long-time annealed samples the high field maximum shifts to higher values with increased annealing temperature, while in the case of the short time annealed samples, the peaks not only shift to higher values but also become narrower at higher annealing temperature, which means that the majority of domain reversal

phenomenon take place in a narrower band i.e. the shape of the hysteresis curve becomes more rectangular.

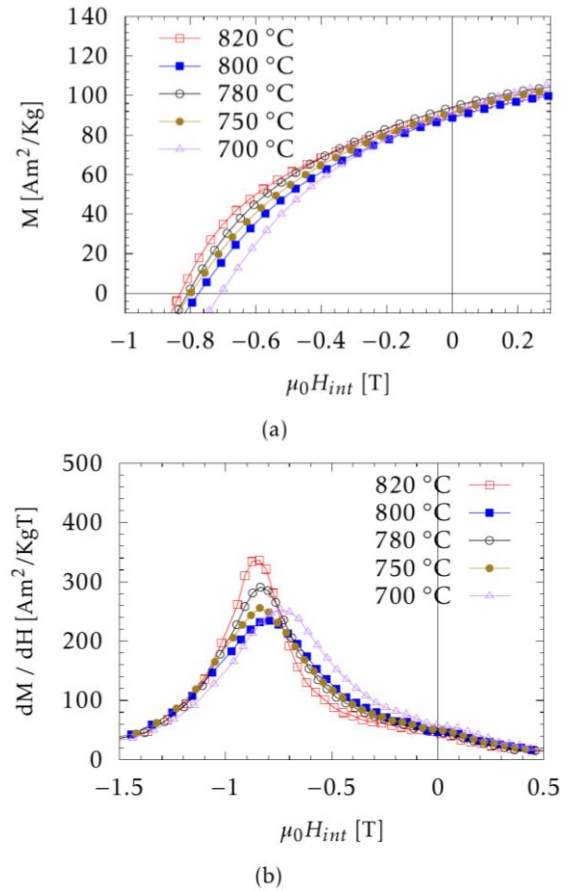


Fig. 5. Demagnetization curves (a) and dM/dH vs H plots (b) for SmCo₅ + 20 wt% α-Fe nanocomposites 6 h MM and annealed at 700 - 820 °C for 1.5 min (color online)

Table 1. Summary of magnetic characteristics for SmCo₅ + 20wt% α-Fe nanocomposite samples

Annealing		H_c	M_r	$(BH)_{max}$
Temperature [°C]	Time [min]	T	Am ² /Kg	kJ/m ³
500 °C	90	0.63	90	91
550 °C	90	0.75	91	96
600 °C	30	0.81	94	98
700 °C	1.5	0.71	91	89
750 °C	1.5	0.80	91	96
780 °C	1.5	0.81	94	103
800 °C	1.5	0.77	88	90
820 °C	1.5	0.83	91	100

The values for H_c , M_r and $(BH)_{max}$ are summarized in Table 1. Here we see that even though we have a high variation in α-Fe grains sizes, Figure 3, in the samples annealed at 500, 550 and 600 °C, the energy product varies only slightly from 91 to 98 kJ/m³. Of course this increase is associated with the increased coercivity from 0.63 T at 500 °C to 0.81 T at 600 °C and remanence (from 90 to 94 Am²/Kg). The relatively small variations in $(BH)_{max}$ is also observed in the short time annealed samples for 1.5 min,

from 89 kJ/m³ at 700 °C to the peak value of 103 kJ/m³ at 780 °C. It should be noted that the higher $(BH)_{max}$ for each set of samples is accompanied by the same H_c , 0.81 T and the same M_r of 94 Am²/Kg. At the same time, the short time annealed sample has a 5% higher energy product, which can be explained by the increased rectangularity of the demagnetization curves, despite the slightly higher α -Fe grain sizes.

4. Conclusions

In the case of SmCo₅ + 20% Fe nanocomposite samples obtained through mechanical milling, it was shown that both short time annealing and long time annealing lead to a good degree of interphase exchange coupling. However, short time annealing at high temperatures lead to improved rectangularity in the demagnetization curves and a 5% increase in the energy product of 103 kJ/m³. This increase is assumed to be due to an increase in the crystallinity of the hard magnetic phase. The short time annealing is consequently preferable. These results are encouraging with respect to the transferal of such annealing regimes to an SPS synthesis route where higher temperatures also lead to higher sample densities.

Acknowledgments

We acknowledge the financial support from the UEFISCDI, Romanian Ministry of Research, Innovation and Digitization, grant PN-III-P2-2.1-PED-2019-4696

References

- [1] J. M. D. Coey, Eng. J. **6**, 119 (2020).
- [2] R. Skomski, P. Manchanda, P. K. Kumar, P. K. Kumar, B. Balamurugan, A. Kashyap, D. J. Sellmyer, IEEE Trans. Magn. **49**, 3215 (2013)
- [3] A. Eldosouky, I. Škulja, J. Magn. Magn. Mater. **454**, 249 (2018).
- [4] M. D. Kuz'min, K. P. Skokov, H. Jian, I. Radulov, O. Gutfleisch, J. Phys.: Condens. Matter **26**, 064205 (2014)
- [5] E. F. Kneller, R. Hawig, IEEE Trans. Magn. **27**, 3588 (1991).
- [6] J. S. Jiang, S. D. Bader, J. Phys. Condens. Matter **26**, 064214 (2014)
- [7] R. Skomski, J. M. D. Coey, IEEE Trans. Magn. **29**, 2860 (1993)
- [8] Q. Wu, J. Li, P. Zhang, M. Pan, H. Ge, Int. J. Electrochem. Sci. **14**, 4318 (2019)
- [9] Q. Chen, B. M. Ma, B. Lu, M. Q. Huang, D. E. Laughlin, J. Appl. Phys. **85**, 5917 (1999)
- [10] R. Hirian, O. Isnard, V. Pop, J. Optoelectron. Adv. M. **21**, 618 (2019).
- [11] R. Hirian, A. Bolinger, O. Isnard, V. Pop, Powder Metall. **61**, 1 (2018).
- [12] D. W. Hu, M. Yue, J. H. Zuo, R. Pan, D. T. Zhang, W. Q. Liu, J. X. Zhang, Z. H. Guo, W. Li, J. Alloy. Compd. **538**, 173 (2012)
- [13] S. Tao, Z. Ahmad, P. Zhang, M. Yan, X. Zheng, J. Magn. Magn. Mater. **437**, 62 (2017)
- [14] L. Z. Zhao, Q. Zhou, J. S. Zhang, D. L. Jiao, Z. W. Liu, J. M. Greneche, Mater. Des. **117**, 326 (2017)
- [15] N. V. Rama Rao, R. Gopalan, M. Manivel Raja, V. Chandrasekaran, D. Chakravarty, R. Sundaresan, R. Ranganathan, K. Hono, J. Magn. Magn. Mater. **312**, 252 (2007)
- [16] R. Hirian, B. V. Neamțu, A. Ferenczi, O. Isnard, I. Chicinaș, V. Pop, Rom. J. Phys. **65**, 603 (2020)
- [17] P. L. Niu, M. Yue, J. X. Zhnag, D. T. Zhnag, Powder Metall. **20**, 219 (2007)
- [18] A. M. Gabay, G. C. Hadjipanayis, M. Marinescu, J. F. Liu, J. Appl. Phys. **107**, 17 (2010)
- [19] V. Neu, S. Sawatzki, M. Kopte, Ch. Mickel, L. Schultz, IEEE Trans. Magn., **48**, 3599 (2012)
- [20] V. Pop, O. Isnard, I. Chicinaș, D. Givord, J. Mag. Magn. Mater., **310**, 2489 (2007)
- [21] S. An, W. Li, K. Song, T. Zhang, C. Jiang, J. Mag. Magn. Mater. **469**, 113 (2019)
- [22] V. Pop, E. Dorolti, C. Vaju, E. Gautron, O. Isnard, J. M. Le Breton, I. Chicinas, Rom. J. Phys. **55**, 127 (2010)
- [23] J. M. Le Breton, R. Larde, H. Chiron, V. Pop, D. Givord, O. Isnard I. Chicinas, J. Phys. D: Appl. Phys. **43**, 085001 (2010)
- [24] P. Scherrer, Nachr. Ges. Wiss. Goettingen, Math.-Phys. Kl. **1918**, 98 (1918).
- [25] R. Hirian, [dissertation]. Cluj-Napoca (Romania): Babes-Bolyai University; (2017) url: https://rei.gov.ro/teza-doctorat-document/840875e7360b3411b4-22.Teza_HirianRazvan.pdf

*Corresponding author: razvan.hirian@ubbcluj.ro